Sigma Journal of Engineering and Natural Sciences
Web page info: https://sigma.yildiz.edu.tr
DOI: 10.14744/sigma.2024.00000

Research Article

Development and application of the truss method on masonry walls to determine the in-plane behavior: A parametric study

Yunus GÜNER[1,*], Ayhan NUHOĞLU[2]

[1]Department of Civil Engineering, Ege University, Izmir, 35100, Türkiye; Department of Civil Engineering, Aydın Adnan Menderes University, Aydın, Türkiye
[2]Department of Civil Engineering, Ege University, Izmir, 35100, Türkiye

ARTICLE INFO

Article history
Received: 03 July 2023
Revised: 12 September 2023
Accepted: 13 November 2023

Keywords:
Capacity Curve; Damage Formation; In-Plane Behavior; Masonry Wall, Simplified Truss Model, The Inclination Angle

ABSTRACT

Determination of the capacity curve and structural behavior of masonry structures is a challenge. While consistent results can be obtained through detailed numerical approaches, the process becomes more complex. Therefore, simplified approaches come to the fore for analysis. This study focuses on this point and proposes a new method that uses a truss model to determine the in-plane behavior of masonry structures. In the development of the proposed method, several important parameters such as the inclination angle, cross-sectional area, mesh size and material parameters are considered. This study specifically conducts a parametric analysis to determine the effect of different angle values on the results. The material model, which employs a macro modeling approach, was adopted from the literature and held constant during the numerical analysis; thus, its effects were excluded from the scope of this study. Variable conditions include mesh size, aspect ratio, compression stress level, and the inclination angle. A series of experimental tests on masonry walls was selected as the reference model, and a numerical model was created using the proposed approach. A total of seventy-two numerical analyses were performed. Consequently, the results were evaluated, and recommendations were made regarding the application of the new model.

Cite this article as: Güner Y, Nuhoğlu A. Development and application of the truss method on masonry walls to determine the in-plane behavior: A parametric study. Sigma J Eng Nat Sci 2024;42(5):1542–1554.

INTRODUCTION

In masonry structures, obtaining precise results often requires conducting detailed tests in both field and laboratory settings, and subsequently transferring the gathered data to software. This process can be labor-intensive and susceptible to potential errors, so necessitating the involvement of qualified personnel. As an alternative, simplified approaches provide more practical and cost-effective solutions. Hence, a new method is proposed. The development process is handled systematically, and the essential parameters are thoroughly discussed within the context of this study.

Simplified approaches aren't just limited to the scope of this study; various alternative suggestions have been

*Corresponding author.
*E-mail address: yunus.guner@adu.edu.tr

This paper was recommended for publication in revised form by Editor-in-Chief Ahmet Selim Dalkilic

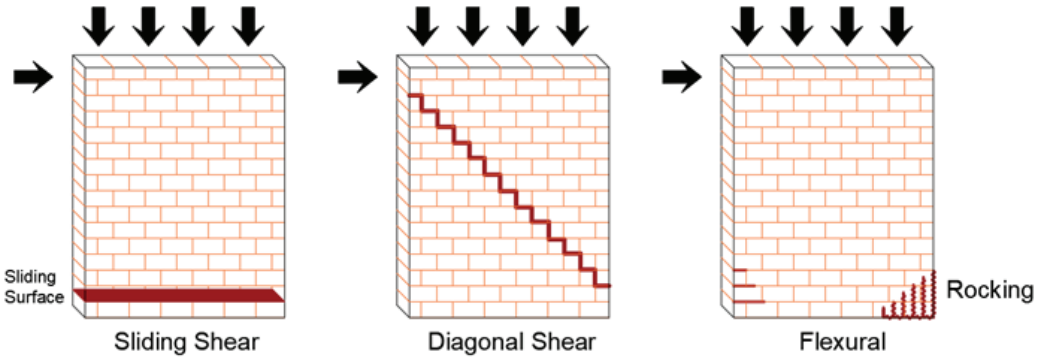

Figure 1. Typical failure modes under in-plane loading.

introduced in other studies. Some of the prominent approaches are the equivalent frame [1] and strut-and-tie [2] models. Furthermore, researchers have proposed various methods, particularly hybrid ones [3,4].

The calculation method employed in the proposed approach relies on truss elements, which have a well-established foundation. Truss elements not only facilitate the creation of a numerical model but also reduce computational effort due to their capacity for carrying only axial loads. While this method finds widespread application in defining the behavior of reinforced concrete structural elements [5,6], its use is limited in masonry structures. In the literature, researchers have predominantly focused on investigating in-plane behavior [7-9], with only a limited number of studies addressing out-of-plane behavior [10,11]. Additionally, one paper delved into the examination of FRP delamination [12]. Micro or macro approaches and hybrid or truss methods were handled under different boundary conditions in these studies. Each study has accuracy or error rates depending on its own acceptance.

The proposed approach utilizes the macro modeling strategy and truss elements in the vertical, horizontal and diagonal directions to create a numerical model. Analyses are carried out using software developed in Python, which includes capabilities for material and geometric nonlinear analysis. Finally, the analysis yields the capacity curve, damage formation, and failure mechanism as results.

In the literature, an inclination angle of 45^0 was commonly used to create the masonry truss model [12-14]. However, regarding reinforced concrete elements such as column and beam, it is observed that the angle is calculated based on the compression stress level and tension capacity [14]. To date, no alternative methods for determining angle values have been explored for masonry structures. Therefore, this study focuses on this topic under alternative conditions. It is well-known that masonry units exhibit high compression capacity but low tensile strength. Consequently, the calculated inclination angle is often significantly greater than 45^0. The results are represented comparatively at the end of this paper.

The validation of the proposed approach is provided considering the in-plane behavior of masonry walls (Figure 1). An experimental test series with two aspect ratios was selected from the literature [15-17]. Initially, the truss model was created with 45^0 inclination angle and compared with both experimental and numerical [18] results. Then, alternative conditions were tested on the truss model. Finally, the effects of the inclination angle were discussed, and the general evaluation was provided.

Following an overview of the challenges posed by existing methods, the proposed approach is briefly described. Its primary goal is to mitigate various problems, including the definition of boundary conditions, variability in material parameters, and software-related challenges commonly encountered when determining the behavior of masonry structures, while also achieving a quicker solution. Rather than seeking an exact numerical solution, the approach facilitates the analysis of alternative conditions and the evaluation of the structure's load-bearing capacity within a confidence interval. The simplification issue has been explored in various studies, but the proposed approach has not yet been addressed. In this study, a parametric study was conducted to incrementally develop the final model and examine the impact of the inclination angle on both the model and the results. As the software continues to evolve, it may also be possible to address dynamic effects such as earthquakes [19] and predict potential damages in advance [20].

MODEL DESCRIPTION

Each truss element connects two nodes, whose rotation are released, and thus only has two degrees of freedom at any in-plane node. It can assume one of three directions: vertical, horizontal or diagonal. Depending on its direction, material parameters and cross-sectional area may vary. The modeling strategy is explained in the following subsections.

Materials

This issue can be quite complicated in masonry structures. Identifying variable material properties in each

structure is a laborious process that requires various laboratory experiments. Several studies have also evaluated material effects [21,22]. The proposed approach aims to simplify this process and reach conclusions with just a few key parameters.

Detecting the nonlinear behavior of a material can be also quite complex, influenced by factors such as fracture energy and pattern. Various studies have explored different materials and conditions [23-27]. In the proposed approach, nonlinear behavior is characterized by the stress-strain curve, making it more understandable and simpler.

In the numerical approach, macro modeling is preferred to simplify material behavior, as shown in Figure 2. Each truss element has different compression and tensile capacities in its axial direction. Vertical or diagonal element uses either compression or tension regions depending on its axial load while transverse element utilizes the shear region instead of tension. Compression and tension behaviors of the material model are derived from an alternative study [9], which is similar to models proposed in other studies [28,29].

In the material model, E_c, f_{tm}, $\in_{tcr}$, $\in_{tu}$, f_{cm}, $\in_{ccr}$, $\in_{cu}$ symbols represent initial compression elastic modulus, maximum tensile strength, cracked tensile strain, ultimate tensile strain, maximum compression strength, cracked compression strain and ultimate compression strain, respectively. The ultimate/first crack tensile and compression strains of a masonry unit are assumed as per Eqs. 1-3.

Determining the shear region is more challenging but crucial for horizontal stability. It is defined as a bi-linear curve, with the maximum unit deformation is accepted as 0.008 [30]. If possible, the maximum shear strength, τ_u, should be determined through an experimental test. Otherwise, the Mohr-Coulomb formula can be used. Here, the residual shear strength is assumed to be nearly equal to the maximum shear strength.

Colors on the material model indicate unit deformation regions developing in the truss elements. They facilitate the evaluation of damage formation and determination of the failure mechanism. After reaching the maximum unit deformation, the element no longer carries any load, and the elastic modulus becomes equal to 10^{-9}.

$$\in_{tcr} = \frac{f_{tm}}{E_c} \tag{1}$$

$$\in_{ccr} = \frac{f_{cm}}{E_c} \tag{2}$$

$$\in_{cu} = 2.75 \times \frac{f_{cm}}{E_c} \tag{3}$$

Inclination Angle

One of the important parameters for defining geometry is the inclination angle, Θ_d. Typically, it is considered perpendicular to the principal stress direction. However, in masonry structure applications, it is commonly accepted as 45^0, making the study's focus on the effects of this angle particularly significant.

The angle primarily effects the cross-sectional area of the diagonal truss element, resulting in changes to the load-bearing capacity of the model. Additionally, it influences the height of the vertical truss element. To determine the angle, a simple procedure was mentioned by Gargari [14]. The stress state is illustrated in Figure 3, and the necessary equations are provided in Eqs. 4-6. σ and τ symbols represent uniform compressive and shear stresses,

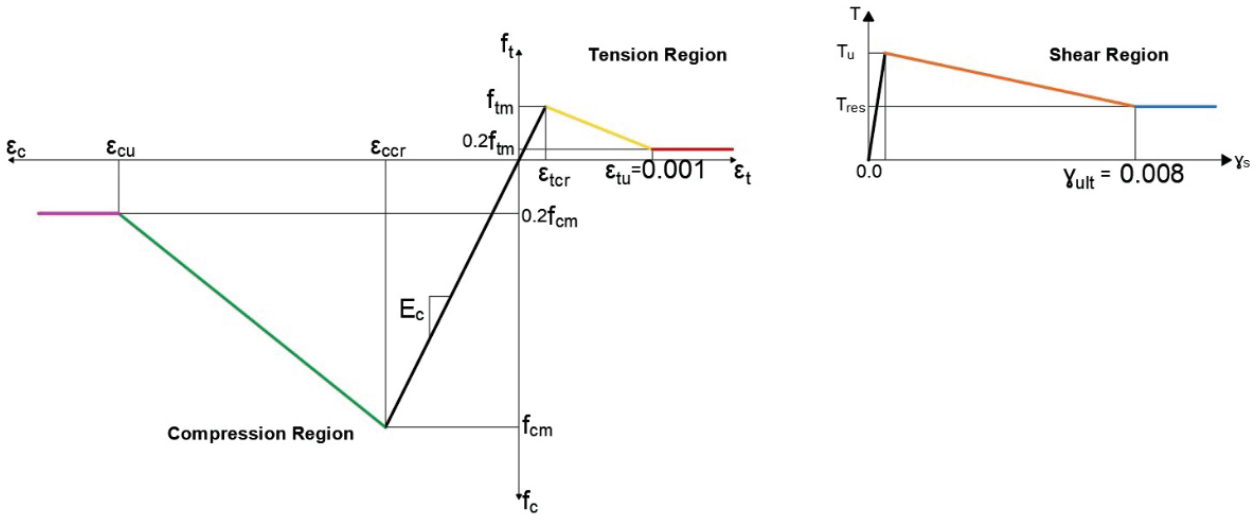

Figure 2. Material model of masonry unit.

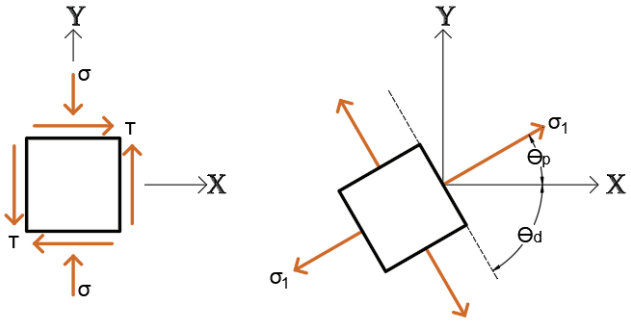

Figure 3. Stress state for determining the inclination angle of diagonal elements.

respectively. The tensile strength, f_t, is equal to the maximum principal stress, σ_1, as diagonal cracking occurs when this threshold is exceeded.

$$\sigma_1 = f_t = \frac{\sigma}{2} + \sqrt{\frac{\sigma^2}{4} + \tau^2} \tag{4}$$

$$tan(2\theta_p) = \frac{2\tau}{\sigma} \tag{5}$$

$$\theta_d = 90^0 - \theta_p \tag{6}$$

Geometry

The method used for determining the cross-sectional areas of truss elements, originally specified for reinforced concrete members (RCM) in the literature [6], was adapted for masonry structures as a result of testing alternative conditions such as full or half cross-sectional areas. The main difference is the use of semi-area in the truss elements, as illustrated in Figure 4. A similar suggestion was also made for RCM by Demirtaş [31].

Change in the inclination angle affects the effective width (D_{eff}). To address this, an alternative approach was employed, ensuring that the total area remains constant for each angle value. Initially, the sum of the cross-sectional area of diagonal elements is determined based on their orientations (vertical or horizontal). Then, the relevant wall cross-sectional area is calculated, and the difference is distributed to vertical or horizontal elements. This ensures that the sum of the cross-sectional areas from the diagonal and vertical/horizontal elements equals that of the wall.

The horizontal width, M, remains constant for each angle, while the height, V, varies regarding the angle. As a result, there may be slight variations in the total height, H, in the parametric study, but these minor size differences do not significantly affect the result [32].

The mesh size equals the horizontal width, M, and acts on determining the D_{eff} along with the angle value. Moreover,

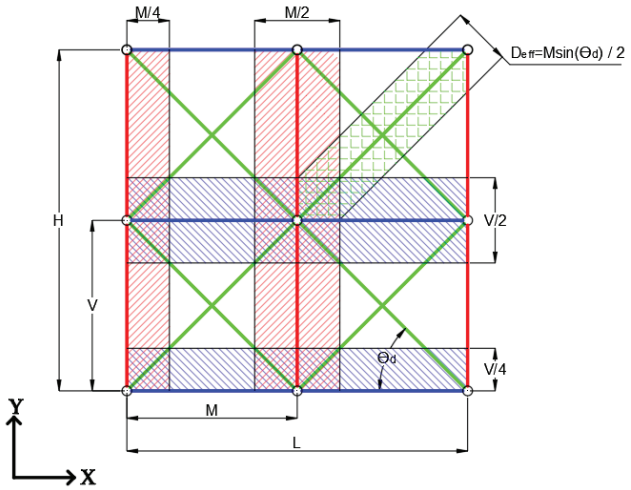

Figure 4. Methodology for determining cross-sectional areas of truss elements.

it is clear that there is a relationship between mesh size and material parameters, but it has not been clearly established yet. Therefore, material parameters are assumed to be constant, and a few mesh sizes are checked through numerical analysis to determine an optimum value.

Failure

In this study, one of the primary focuses is on defining failure mechanisms and understanding crack development. The typical failure modes illustrated in Figure 1 are represented through the proposed truss model. Sliding shear is defined as tension damage developing simultaneously in both the vertical and diagonal elements. Diagonal shear occurs specifically in the diagonal elements due to tension damage. Moreover, plastic deformation may sometimes develop in the horizontal element exceeding the maximum shear strength. Thus, it can be predicted that greater diagonal damage will occur. Last one, rocking, is described as compression damage occurring in the vertical and diagonal elements. The transverse elements typically play a crucial role in providing horizontal stability.

In addition to creating numerical model and defining material parameters, accurately representing loading and boundary conditions is very important for determining crack development. While boundary conditions may vary considering any sample, the loading procedure remains consistent. At first, axial and dead loads are applied to the model (Step 1). The model is then subjected to horizontal monotonic loading (Step 2).

To apply loads other than dead load, a steel/concrete loading frame is used. This frame is created in two rows using the proposed method and placed at the top of the wall. It allows for the equal distribution of loads across the model. Additionally, nodes are added to the intersection points of the diagonal elements in the top row for improved load distribution.

Flowchart

The software that is able to solve nonlinear behavior is developed using Python. The solution algorithm, outlined in the flowchart in Figure 5, begins with inputs such as geometric and material properties, loading and boundary conditions, and node coordinates. Subsequently, loads are applied step by step, and a pushover analysis is carried out.

At each iteration, the global stiffness matrix is determined and solved with the global load matrix together; therefore, displacements developing at nodes and strain in frame elements are calculated. The new node coordinates are updated for the next iteration, and thereby accounting for the effect of geometric movement in the analysis. In the material nonlinear phase, the total strain value is considered. Based on this, the new elastic module is calculated according to the stress-strain curve mentioned in Figure 2.

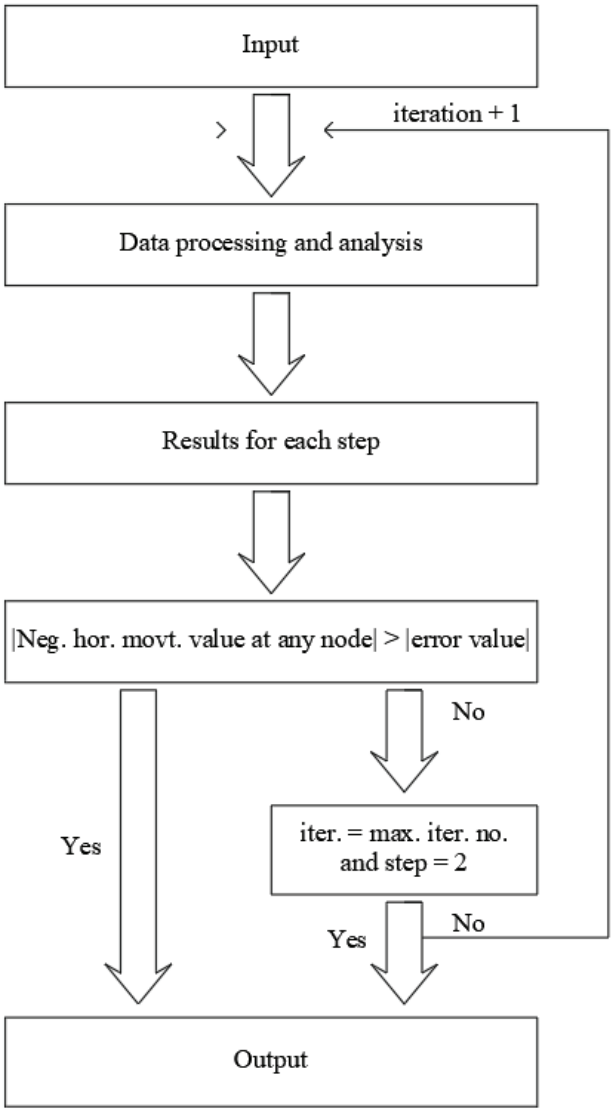

Figure 5. The flowchart.

In the red, magenta and blue lines of the curve, the elastic modulus is assumed to be approximately zero.

Cumulative displacement at any node is compared with the initially accepted negative error value to determine whether the analysis continues. The number of steps and iterations is also checked. Finally, this process yields the capacity curve, failure mode, and crack development.

Validation

This paper focuses on two masonry walls constructed from stone to validate the proposed truss model and explore alternative conditions in the parametric study (Figure 6). In the experimental model, the wall thickness is 320 mm, and the top rotation is restricted. Material parameters determined experimentally are listed in Table 1. The elastic modulus was calculated considering the compression stress-strain curve of the wallet. However, it is not always sufficient to describe the stiffness of the structure due to factors such as geometric configuration, boundary conditions, and non-homogeneous form [18]. To enhance the reliability of material parameters and determine a structure's initial stiffness, non-destructive methods such as operational modal analysis can be preferred [33]. In the proposed model, the elastic modulus for the CT series was updated with minimal deviations from the experimental results (Table 2).

The maximum shear strength, τ_u, is determined using the Mohr-Coulomb formulation (Eqn. 7). Cohesion, c, is not specified in the literature, so it is assumed to be two times the tensile strength of the material, denoted as $2 * f_{tm}$. This assumption is based on a formula suggested in another parametric study on rubble stone walls conducted by Pereira et al. [34]. The friction coefficient, μ, is recommended as 0.4 by the Turkish Building Earthquake Code [35]. Lastly, the pre-compression (σ_v) depends on axial stress level. The residual shear strength is assumed to be almost equal to the maximum value.

$$\tau_u = c + \mu\sigma_v \tag{7}$$

Firstly, the truss model with 45^0 inclination angle was created using two different mesh sizes (M= 150 and 250 mm). While a fixed support at the lowest nodes was applied, the nodes at the loading frame were connected to each other using the Master-Slave method. The goal here is not to obtain the best overlap at each test. Instead, it is to determine the optimum model parameter (mesh size) that yields consistent results across all tests. In the parametric study, all numerical results will be compared within their respective categories.

The capacity curves obtained from the finite element analysis, the experimental test, and the proposed truss model are shown in Figure 7. A load-controlled method is applied in the truss model, and the capacity curve exhibits only an increase at each iteration. In other words, there is no load decline after reaching the peak. The 250 mm mesh

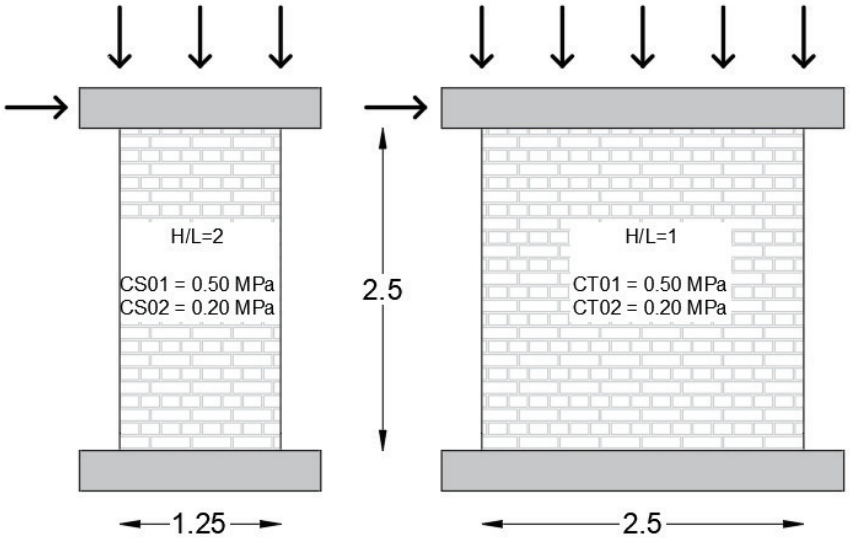

Figure 6. The wall samples (m).

Table 1. Material parameters (MPa) (G Shear modulus)

	G	fcm	ftm
Magenes et al. [16]	840	3.28	0.137
Araujo [18]	-	3.28	0.140
Truss model	840	3.28	0.137

Table 2. Elastic modulus (MPa)

	CS01	CS02	CT01	CT02
Magenes et al. [16]	2550	2550	2550	2550
Araujo [18]	1500	2000/1100	1000	800
Truss model	2550	2550	2000	2000

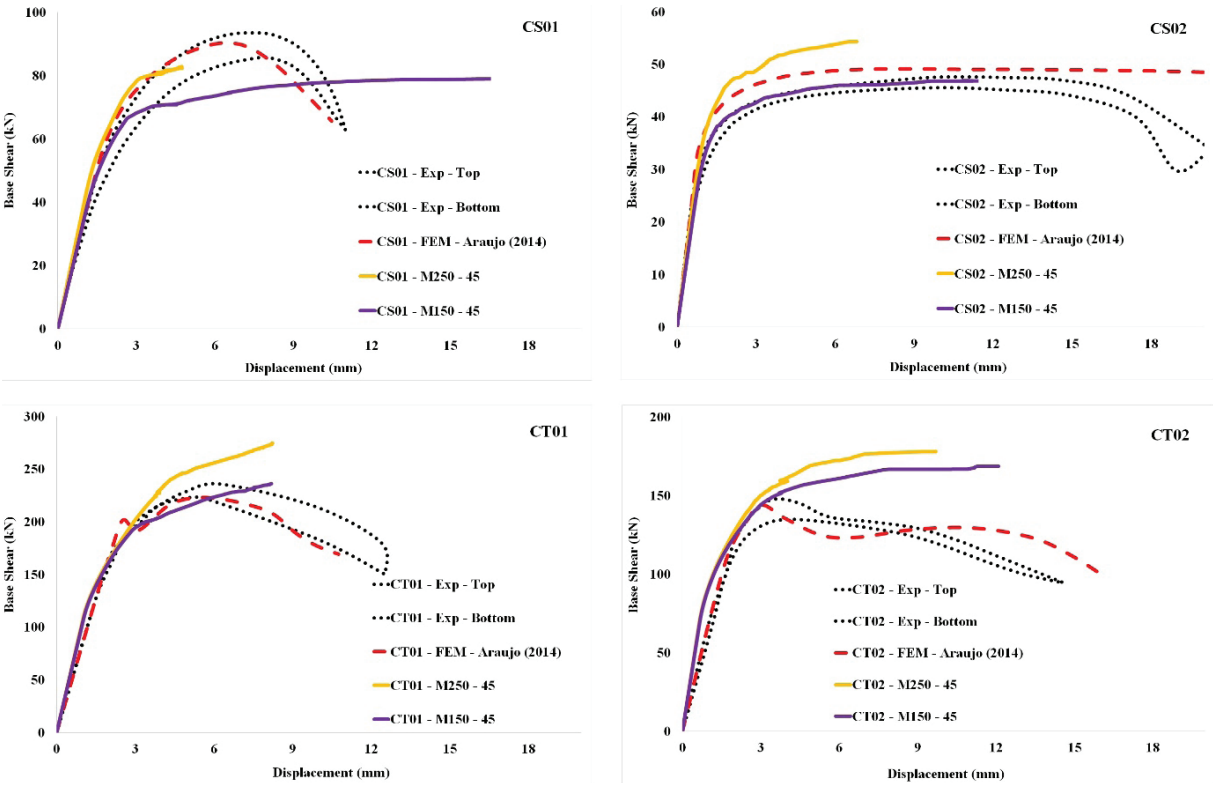

Figure 7. The capacity curves.

size has the highest capacity among all the analyses except for CS01. At 150 mm, while the curve is below the expectation in CS01, it is slightly above in CT02. Nevertheless, it is a more suitable option. Moreover, smaller mesh sizes represent the damage distribution better.

Detection of crack formation and failure modes is as important as the harmony of the capacity curve. Failure modes are presented in Table 3, and a high degree of similarity is observed. Crack formation is compared with the numerical model and investigated separately at each wall. At CS01, while flexure and shear failures are both influential at the peak load, shear failure leads to collapse in the final stage. CS02 demonstrates an obvious flexural failure, with openings in the lower left and upper right corners of the wall. Diagonal cracking dominates at CT01 because of the high axial stress level. At CT02, flexural behavior is more pronounced initially due to lower axial loading, but after reaching peak load, shear failure significantly affects the wall. The proposed novel model exhibits a similar pattern of damage development (Figure 8). It isn't observed that damage modes, such as CS01 and CT02, change because unit deformation value is not scaled in the truss model. For example, at CS01, diagonal cracking spreads throughout the entire model, but openings at the corners are still visible. Similarly, flexure failure turns into shear at CT02. This progression is evaluated through gradual damage development (Figure 9). Initially, flexural behavior is observed, and then it turns into shear failure, consistent with the findings of the finite element analysis. Regardless of the extent of diagonal damage, the flexural damage in the corners still continues to appear.

Table 3. Failure modes

	CS01	CS02	CT01	CT02
Magenes et al. [16]	Shear	Flexure and Shear	Shear	Shear
Araujo [18]	Shear	Flexure	Shear	Shear
Truss model	Shear	Flexure	Shear	Shear

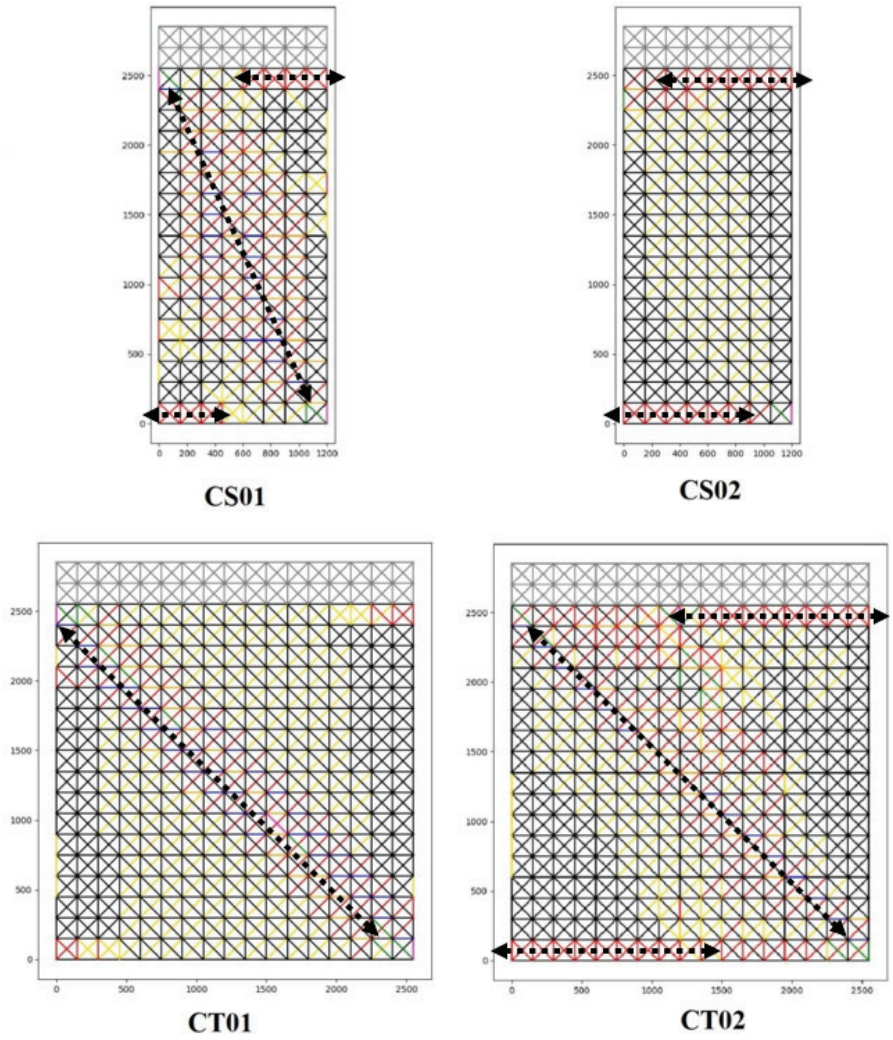

Figure 8. The damage distribution on the truss model considering the stress-strain curve.

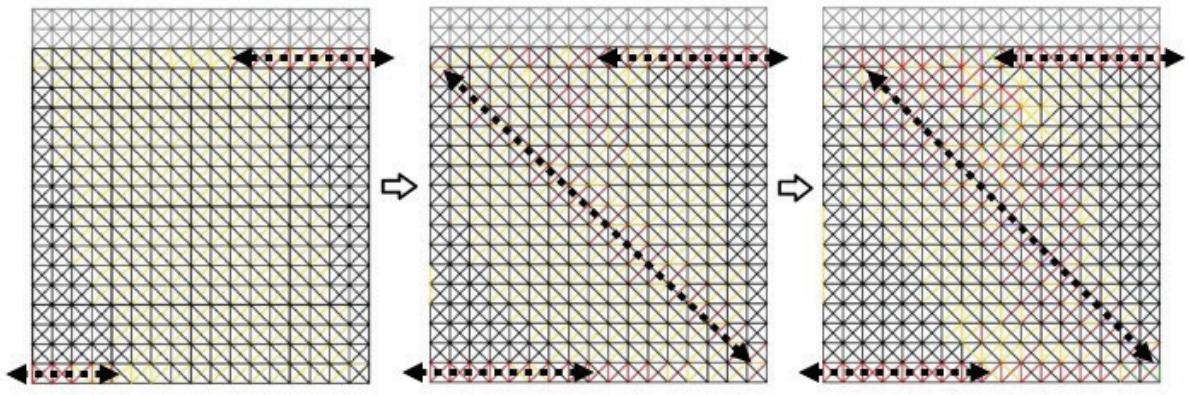

Figure 9. The gradual damage development at CT02.

Comparatively, 45^0 yields highly successful results, especially in accurately determining damage formation and the failure mechanism.

PARAMETRIC STUDY

After comprehensive validation, a parametric study was conducted to understand the effects of the inclination angle on the truss model. Changes in the cross-sectional area of the diagonal elements, depending on the angle, are given in Table 4. Numerous parameters were selected for this study, and 72 analyses were performed. The test samples with an axial load level of 0.35 MPa were designated as CS03 and CT03. The parameters are as follows:

- Inclination angle: 40^0, 45^0, 50^0, 55^0, 60^0 and 65^0
- Mesh size: 150 and 250 mm
- Aspect ratio (H/L): 1.0 and 2.0
- Axial stress level: 0.20, 0.35 and 0.50 MPa

Pre-evaluation

A pre-evaluation was conducted to facilitate result interpretation, and the results were as follows.

- A larger mesh size (250 mm) exhibits greater load-bearing capacity in all analyses, regardless of the boundary conditions. However, the difference between capacities may vary for each analysis.
- Reducing the aspect ratio by half nearly triples the load-bearing capacity. Similarly, an increase in axial stress augments the overall capacity. For instance, these rates average 40% (σ= 0.35 MPa) and 73% (σ= 0.50 MPa) for the CS series with the 150 mm mesh size at three angle values when compared to the 0.20 MPa axial stress level. Furthermore, it is anticipated that the failure mode will transition from flexure to shear with an increase in axial stress.
- For $\Theta_d = 40^0$, the capacity curve inadequately represents the experimental test; hence, there is no need to consider lower angle values. And also in masonry structures, the inclination angle generally exceeds 45^0.
- For $\Theta_d = 60^0$, the capacity curve may align with the literature, but it fails to accurately predict the failure mode and crack development. The dominant cause of damage in the analyses is typically flexural.
- For $\Theta_d = 65^0$, it is observed that both the capacity curve and the failure mode are not determined correctly.

It is observed that increase in the angle results in a flexure-dominated response, with no strength degradation due

Table 4. Cross-sectional areas of diagonal elements (mm^2). (Rates of change are given in parentheses.)

	400	450	500	550	600	650
M150	15427 (-9%)	16971 (0%)	18385 (8%)	19660 (16%)	20785 (22%)	21751 (28%)
M250	25712 (-9%)	28284 (0%)	30642 (8%)	32766 (16%)	34641 (22%)	36252 (28%)

Table 5. The natural period values at 0.50 MPa axial stress level (s). (Rates of change are given in parentheses.)

	400	450	500	550	600	650
CS01	0.149 (-2.0%)	0.152 (0.0%)	0.150 (-1.3%)	0.156 (2.6%)	0.161 (5.9%)	0.167 (9.9%)
CT01	0.114 (-8.1%)	0.124 (0.0%)	0.123 (-0.8%)	0.130 (4.8%)	0.138 (11.3%)	0.150 (21.0%)

to shear damage in column elements [14]. This finding aligns with the results presented in this paper. Therefore, these three angles (Θ_d =40^0, 60^0, 65^0) were excluded from the overall assessment.

When evaluating initial stiffness based on the dominant natural period values, the results indicate that the period increases with a rise in the angle. In other words, the initial stiffness of the model, especially at Θ_d = 60^0 and Θ_d = 65^0, decreases. In Table 5, the dominant natural period values of CS01 and CT01 under a 0.5 MPa axial stress level are given.

General evaluation

Figures 10-11 present the capacity curves for two mesh sizes: 150 and 250 mm. While not all interpretations are supported by all analyses, some general trends emerge:

- The curves in the CS series exhibits greater consistency, possibly due to a limited maximum load value.
- Truss model with the 250 mm mesh size generally exhibits a higher load-bearing capacity than expected, save for CS01.
- In 150 mm mesh size, models with angles of 50^0, 45^0 and 55^0 have the maximum load-bearing capacity in eight, three and one analyses, respectively.

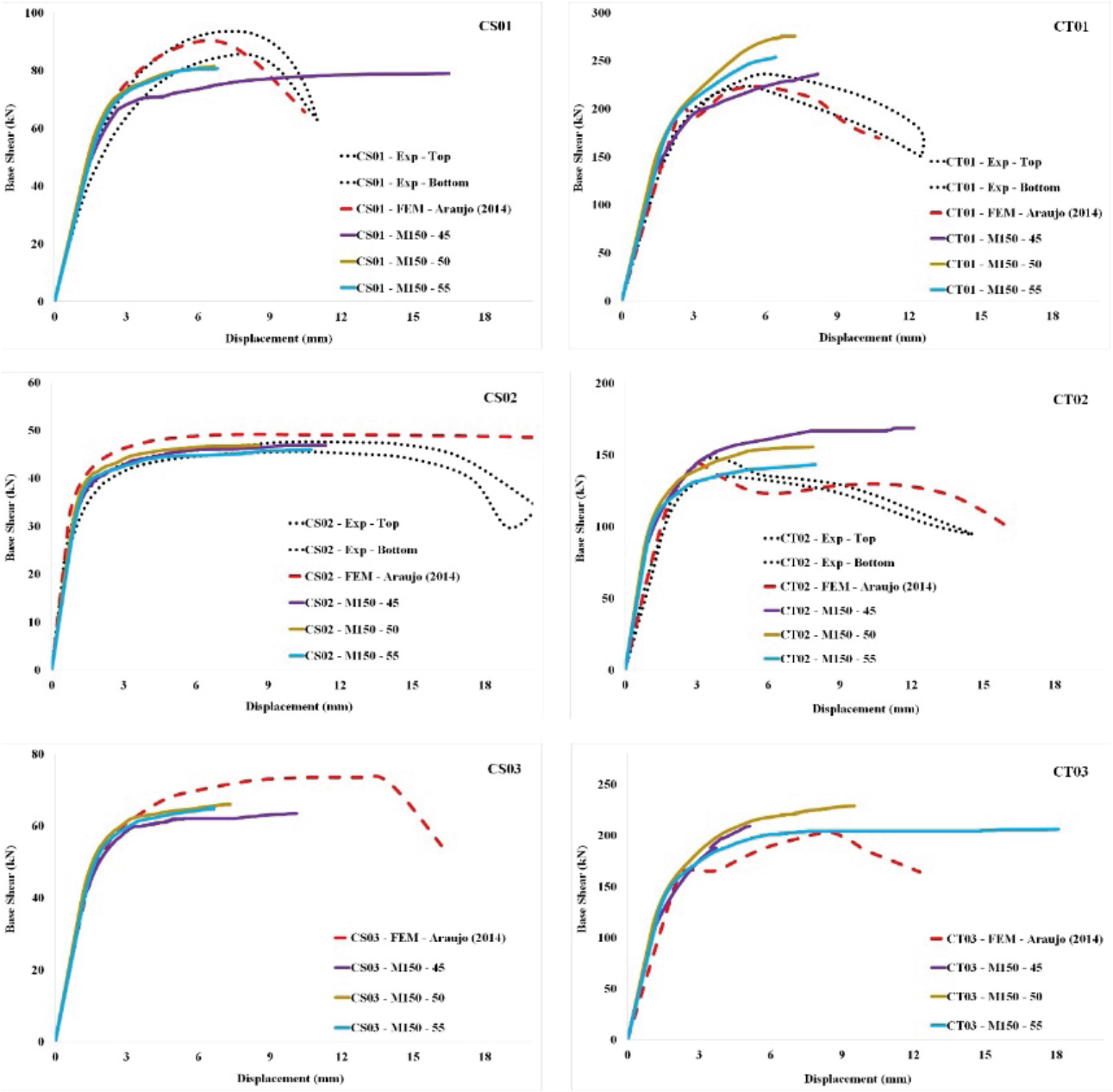

Figure 10. The capacity curves for the 150 mm mesh size.

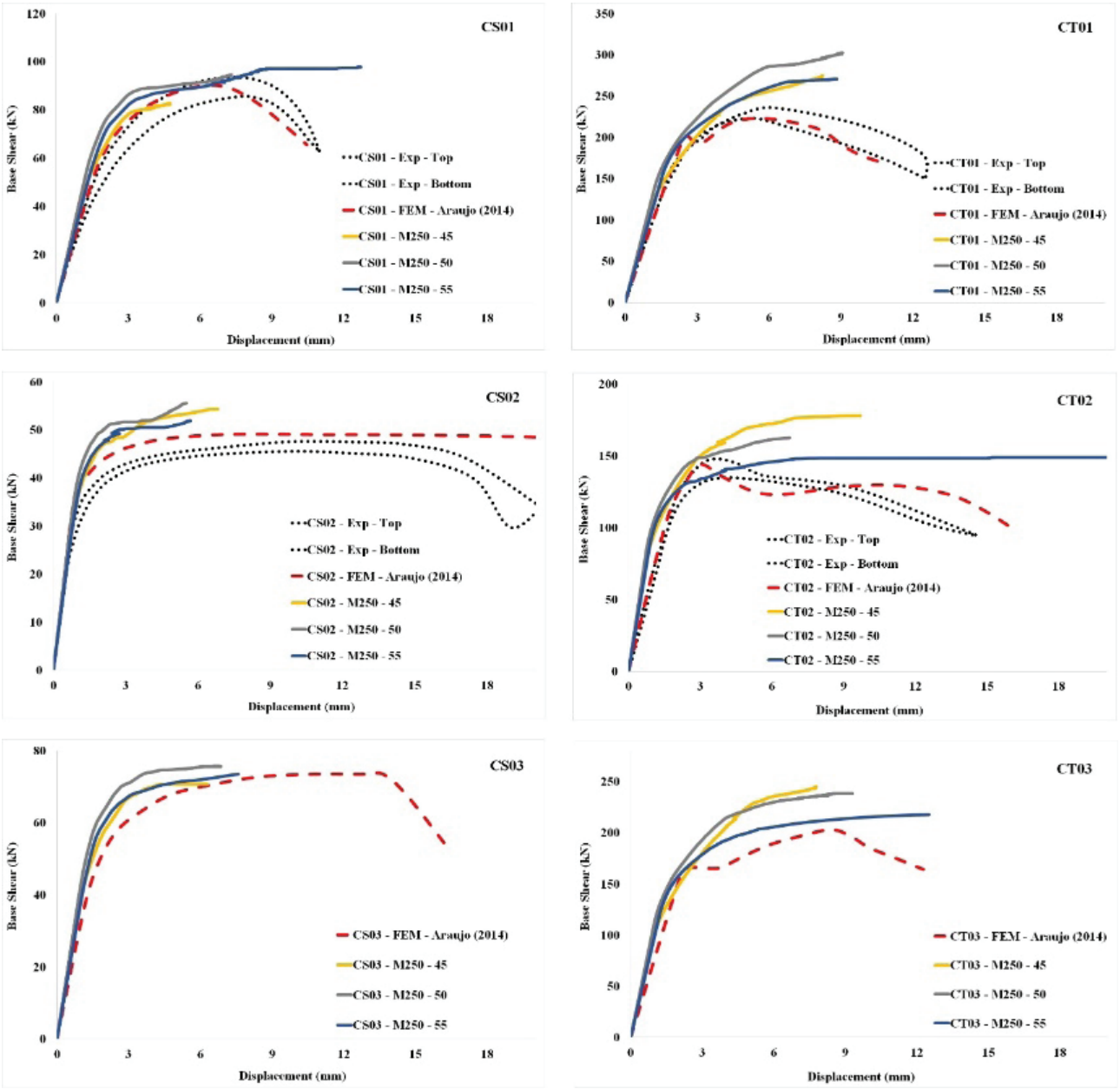

Figure 11. The capacity curves for the 250 mm mesh size.

- As the angle increases, the linear region of the capacity curve tends to be larger, owing to the increased cross-sectional areas of diagonal elements. Consequently, common tension damage in diagonal truss elements is delayed.
- All angle values seem to be compatible, with 55^0 potentially representing an optimal choice. However, a comprehensive evaluation should also consider factors like failure mode and crack formation to avoid potential misinterpretations.

In damage formations, there are important results that can change interpretations. Evaluations are performed with the 150 mm mesh size. Initially, while significant diagonal damage is expected in wall CS01, it could not be detected in the truss models with 50^0 and 55^0 angles due to limited horizontal movement. The damage only develops in the lower left and upper right corners. The same situation is observed for CS03. In the finite element analysis performed by Araujo [18], flexural and shear failure modes occur together. In the proposed model, this behavior is best represented by the 45^0 angle (Figure 12). At CS02, there is general consistency.

In CT01 analyses, it is observed that the shear failure mode becomes in a steeper form with the rise of the angle (Figure 13), and it is more overlapped with the finite element result. However, unexpected major flexural damages also emerge. Although shear failure begins to occur at 55^0

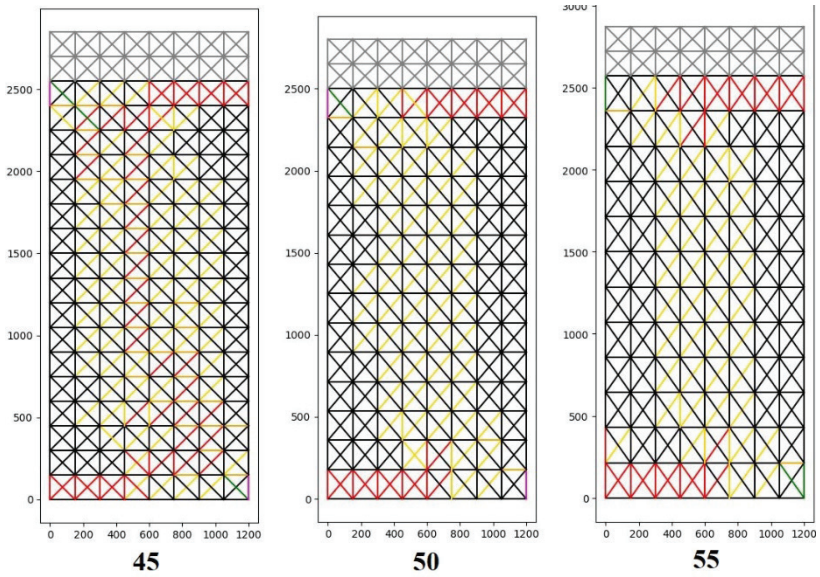

Figure 12. The damage formation depending on the inclination angle (150 mm mesh size – CS03).

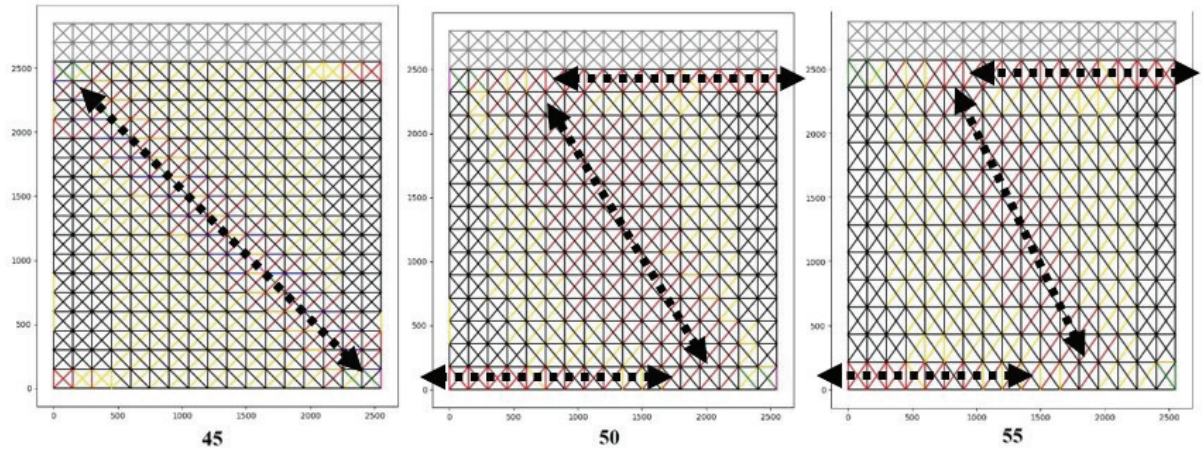

Figure 13. The damage formation depending on the inclination angle (150 mm mesh size – CT01).

in CT02, flexural damage is still dominant. At 50^0, only the flexural failure mode is observed. Finally, in CT03, the situation is similar to CT01. The 45^0 angle usually exhibits the most consistent results for both aspect ratios (CS and CT).

The results obtained with the 250 mm mesh size are generally similar to those obtained with the 150 mm mesh size. However, increasing the mesh size reduces the visibility of damage distribution and complicates result interpretation.

CONCLUSION

This paper focuses on a parametric study to improve a novel method for representing the in-plane behavior of masonry structures. Various alternative conditions are systematically examined to address uncertainties that have not been thoroughly explored in the existing literature.

In masonry structures, tension stress capacity is considerably lower than compression strength, leading to higher inclination angles. For example, the inclination angle values calculated for axial stress levels of 0.50, 0.35 and 0.20 MPa are 65^0, 62^0 and 57^0, respectively. Based on the results of the parametric study, it is recommended that the angle should not be chosen smaller than 45^0 or bigger than 55^0.

An angle of 45^0 is found to be optimal for determining the capacity curve and assessing damage development. However, to enhance result sensitivity, the angle may be varied within the range of 45^0 to 55^0, provided that pre-checks such as crack formation and failure mode are performed.

The proposed method can effectively describe the behavior of masonry structures, particularly as a preliminary analysis tool. However, it's important to note that it may not provide an exact solution, such as micro analysis.

The inclination angle plays a significant role in the determining cross-sectional area of diagonal elements, which, in turn, affects the load-bearing capacity of the numerical approach. Changes in the angle can significantly alter the distribution of cross-sectional areas. For example, increasing the angle from 45^0 to 50^0 results in an approximate 8% increment in the cross-sectional area of the diagonal element. The parameter, D_{eff}, used in this study may be updated to minimize its effect. Additionally, conducting new test series may yield improved results.

AUTHORSHIP CONTRIBUTIONS

Authors equally contributed to this work.

DATA AVAILABILITY STATEMENT

The authors confirm that the data that supports the findings of this study are available within the article. Raw data that support the finding of this study are available from the corresponding author, upon reasonable request.

CONFLICT OF INTEREST

The author declared no potential conflicts of interest with respect to the research, authorship, and/or publication of this article.

ETHICS

There are no ethical issues with the publication of this manuscript.

REFERENCES

[1] Siano R, Sepe V, Camata G, Spacone E, Roca P, Pela L. Analysis of the performance in the linear field of Equivalent-Frame Models for regular and irregular masonry walls. Eng Struct 2017;145:190–210. [CrossRef]

[2] Foraboschi P, Vanin A. Non-linear static analysis of masonry buildings based on a strut-and-tie modeling. Soil Dyn Earthq Eng 2013;55:44–58. [CrossRef]

[3] Verbrugge M. Modelling in-plane behaviour of masonry shear walls through a predefined crack pattern at macro level (master thesis). The Netherlands: Delft University of Technology; 2017.

[4] Kafkas U. Yığma duvar elastik davranışının düzlem çubuk elemanlarla mikro modellemesi (yüksek lisans tezi). Kütahya: Dumlupınar Üniversitesi Fen Bilimleri Enstitüsü; 2015 [Turkish]

[5] Girgin SC, Moharrami M, Koutromanos I. Nonlinear beam-based modeling of RC columns including the effect of reinforcing-bar buckling and rupture. Earthq Spect 2018;34:1289–1309. [CrossRef]

[6] Lu Y, Panagiotou M. Three-dimensional cyclic beam-truss model for nonplanar reinforced concrete walls. J Struct Eng 2014;140:04013071. [CrossRef]

[7] D'Altri AM, de Miranda S. Prediction of flexural drift capacity in masonry walls through a nonlinear truss-based model. Int J Solids Struct 2022; 243:111593. [CrossRef]

[8] Salinas D, Koutromanos I, Leon RT. Nonlinear truss modeling method for masonry-infilled reinforced concrete frames. Eng Struct 2022;262:114329. [CrossRef]

[9] Pirsaheb H, Wang P, Moradi MJ, Milani G. A Multi-Pier-Macro MPM method for the progressive failure analysis of perforated masonry walls in-plane loaded. Eng Fail Anal 2021;127:105528. [CrossRef]

[10] Pirsaheb H, Wang P, Milani G, Habibi M. A Multi-Pier-Macro MPM method for the progressive failure analysis of full scale walls in two way bending. Eng Fail Anal 2022;131:105862. [CrossRef]

[11] Ridwan M, Yoshitake I, Nassif AY. Two-dimensional fictitious truss method for estimation of out-of-plane strength of masonry walls. Construct Build Mater 2017;152:24–38. [CrossRef]

[12] Zhao L, Song Z, Feng H, Zhao M, Pirsaheb H. A Multi Pier (MP) method for the evaluation FRP delamination on flat and curve masonry substrates. Compos Struct 2022; 294:115793. [CrossRef]

[13] Pirsaheb H, Moradi MJ, Milani G. A Multi-Pier MP procedure for the non-linear analysis of in-plane loaded masonry walls. Eng Struct 2020; 212:110534. [CrossRef]

[14] Gargari MM. Development of novel computational simulation tools to capture the hysteretic response and failure of reinforced concrete structures under seismic loads (master thesis). Virginia, USA: The Faculty of The Virginia Polytechnic Institute and State University; 2016.

[15] Magenes G, Morandi P, Penna A. Test results on the behaviour of masonry under static cyclic in plane lateral loads. Enhanced safety and efficient construction of masonry structures in Europe, Project No. Coll - Ct - 2003 - 500291, University of Pavia, 2008.

[16] Magenes G, Penna A, Galasco A, Da Pare M. In-plane cyclic shear tests of undressed double-leaf stone masonry panels, 8th International Masonry Conference 2010, Dresden.

[17] Magenes G, Penna A, Galasco A, Rota M. Experimental characterisation of stone masonry mechanical properties, 8th International Masonry Conference 2010b; 247-56, Dresden.

[18] Araujo ASFF. Modelling of the seismic performance of connections and walls in ancient masonry buildings (phd thesis). Portugal: University of Minho; 2014.

[19] Nayak CB. A state-of-the-art review of vertical ground motion (VGM) characteristics, effects and provisions. Innov Infrastruct Solut 2021; 6:124. [CrossRef]

[20] Işık E, Avcil F, Büyüksaraç A, İzol R, Arslan MH, Aksoylu C, et al. Structural damages in masonry buildings in Adıyaman during the Kahramanmaraş (Turkiye) earthquakes (Mw 7.7 and Mw 7.6) on 06 February 2023. Eng Fail Anal 2023;151:107405. [CrossRef]

[21] Zengin B, Koçak A. The effect of the bricks used in masonry walls on characteristic properties. Sigma J Eng Nat Sci 2017;35:667–677.
[22] Aktan S, Doran B. Constitutive modeling of masonry walls under in-plane loadings. Sigma J Eng Nat Sci 2016;7:165–171. [Turkish]
[23] Reyes E, Galvez JC, Casati MJ, Cendon DA, Sancho JM, Planas J. An embedded cohesive crack model for finite element analysis of brickwork masonry fracture. Eng Fract Mech 2009;76:1930–1944. [CrossRef]
[24] Yuen TYP, Deb T, Zhang H, Liu Y. A fracture energy based damage-plasticity interfacial constitutive law for discrete finite element modelling of masonry structures. Comput Struct 2019;220:92–113. [CrossRef]
[25] Wang H, Dyskin A, Dight P, Pasternak E, Hsieh A. Review of unloading tests of dynamic rock failure in compression. Eng Fract Mech 2020;225:106289. [CrossRef]
[26] Bolat Ç, Bilge G, Gökşenli A. An investigation on the effect of heat treatment on the compression behavior of aluminum matrix syntactic foam fabricated by sandwich infiltration casting. Mater Res 2021;24:e20200381. [CrossRef]
[27] Spetz A, Denzer R, Tudisco E, Dahlblom O. Phase-field fracture modelling of crack nucleation and propagation in porous rock. Int J Fract 2020;224:31–46. [CrossRef]
[28] Nadjai A, O'Garra M, Ali F. Finite element modelling of compartment masonry walls in fire. Comput Struct 2003;81:1923–1930. [CrossRef]
[29] Lourenco PB. Computational strategies for masonry structures (phd thesis). The Netherland: Delft University of Technology; 1996.
[30] Thuyet VN, Deb SK, Dutta A. Mitigation of seismic vulnerability of prototype low-rise masonry building using U-FREIs. J Perform Constr Facil 2018;32:04017136. [CrossRef]
[31] Demirtaş Y, Yurdakul Ö, Avşar Ö. Lattice modelling of substandard RC beam-column joints considering localization issues. Structures 2023;47:2515–2530. [CrossRef]
[32] Güner Y, Nuhoğlu A. Analysis of in-plane behaviour of masonry structures by truss model approach. Süleyman Demirel Univ J Nat Appl Sci 2022;26:479–489. [Turkish] [CrossRef]
[33] Ercan E, Arısoy B, Hökelekli E, Nuhoğlu A. Estimation of seismic damage propagation in a historical masonry minaret. Sigma J Eng Nat Sci 2017;35:647–666.
[34] Pereira JM, Correia AA, Lourenço PB. In-plane behaviour of rubble stone masonry walls: Experimental, numerical and analytical approach. Construct Build Mater 2021;271:121548. [CrossRef]
[35] Turkish Building Earthquake Code. Resmi Gazete 2018; Sayı: 30364 (Mükerrer) [Turkish]